

## Supplemental Information

### Plate Tectonics of Virus Shell Assembly

### and Reorganization in Phage $\Phi 8$ ,

### a Distant Relative of Mammalian Reoviruses

Kamel El Omari, Geoff Sutton, Janne J. Ravantti, Hanwen Zhang, Thomas S. Walter, Jonathan M. Grimes, Dennis H. Bamford, David I. Stuart, and Erika J. Mancini

#### Inventory of Supplemental Information

**Figure S1: Crystal packing the  $\phi 8$  P1 pentamers, related to Figure 1.**

*Figure shows the unusual high solvent content of the  $\phi 8$  P1 crystals.*

**Figure S2: Representative 2fo- $\sigma$  electron density map of  $\phi 8$  P1 contoured at  $1\sigma$ , related to Figure 1.**

*Figure S2 shows the quality of the electron density maps at  $3.7\text{\AA}$  resolution corresponding to the structure presented in this paper.*

**Figure S3: (A,B) Comparison of the crystal structure pentamer (grey) to the procapsid pentamer (green) as obtained by fitting P1 monomers into the 5-fold**

axis of the  $\phi 6$  procapsid cryo-EM reconstruction, related to Figure 4. (C) Interactions between A (green) and B (red) subunits in the expanded capsid.

*Figure S3 panels A and B shows similarities between the pentamers from the crystal structure and the one fitted in the procapsid reconstruction. Panel C shows a close-up view of the interactions of subunits A with subunit B.*

**Figure S4: Presence of pentamers in solution shown by negative-stain EM, related to Figure 5.**

*Figure S4 shows that  $\phi 8$  P1 pentamers are present in solution and suggest they are the building blocks for procapsid assembly.*

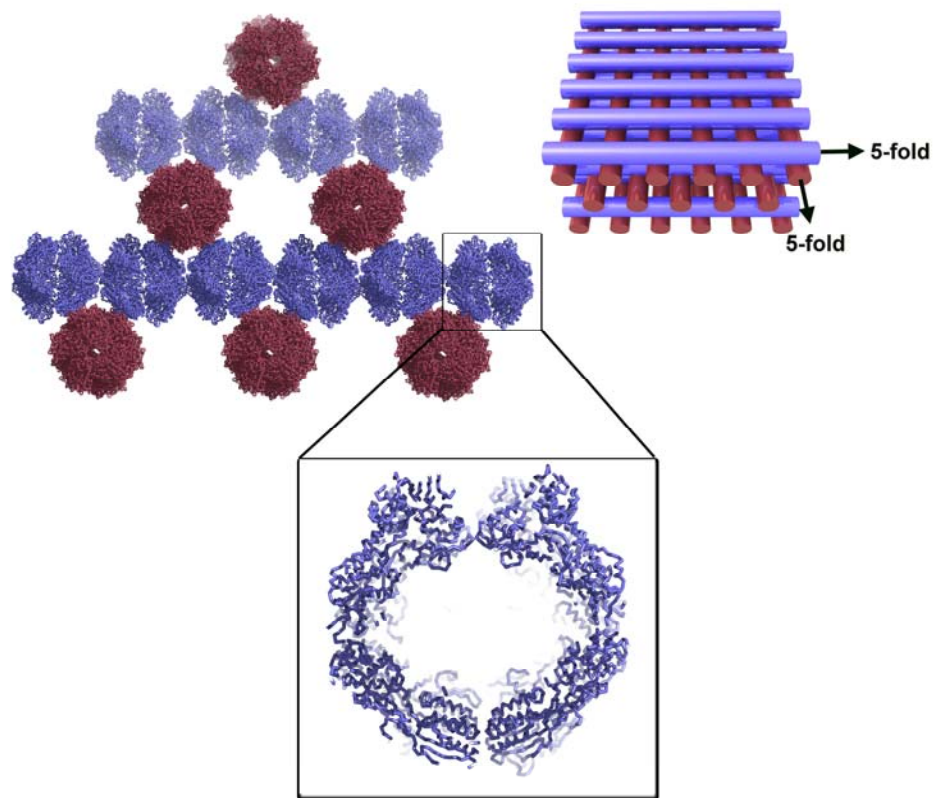


**Figure S1**

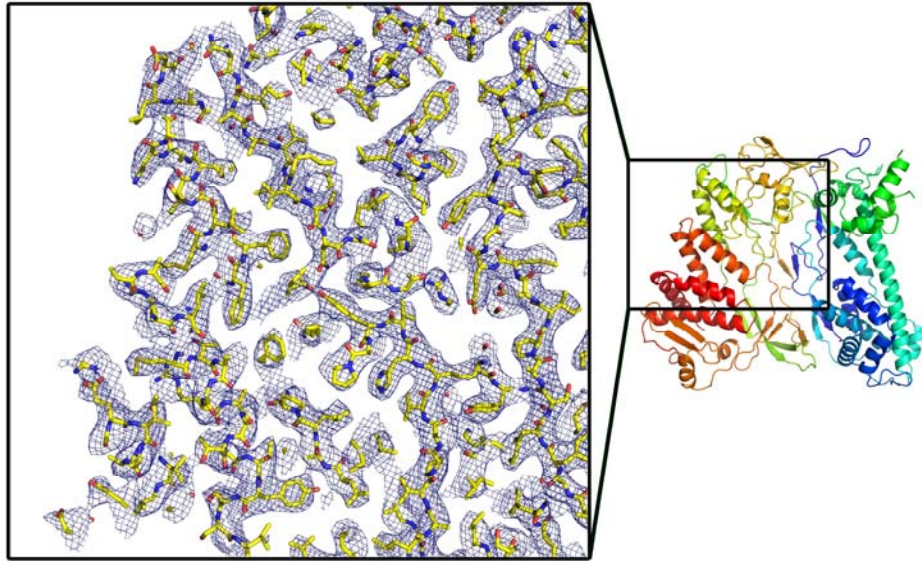


**Figure S2**

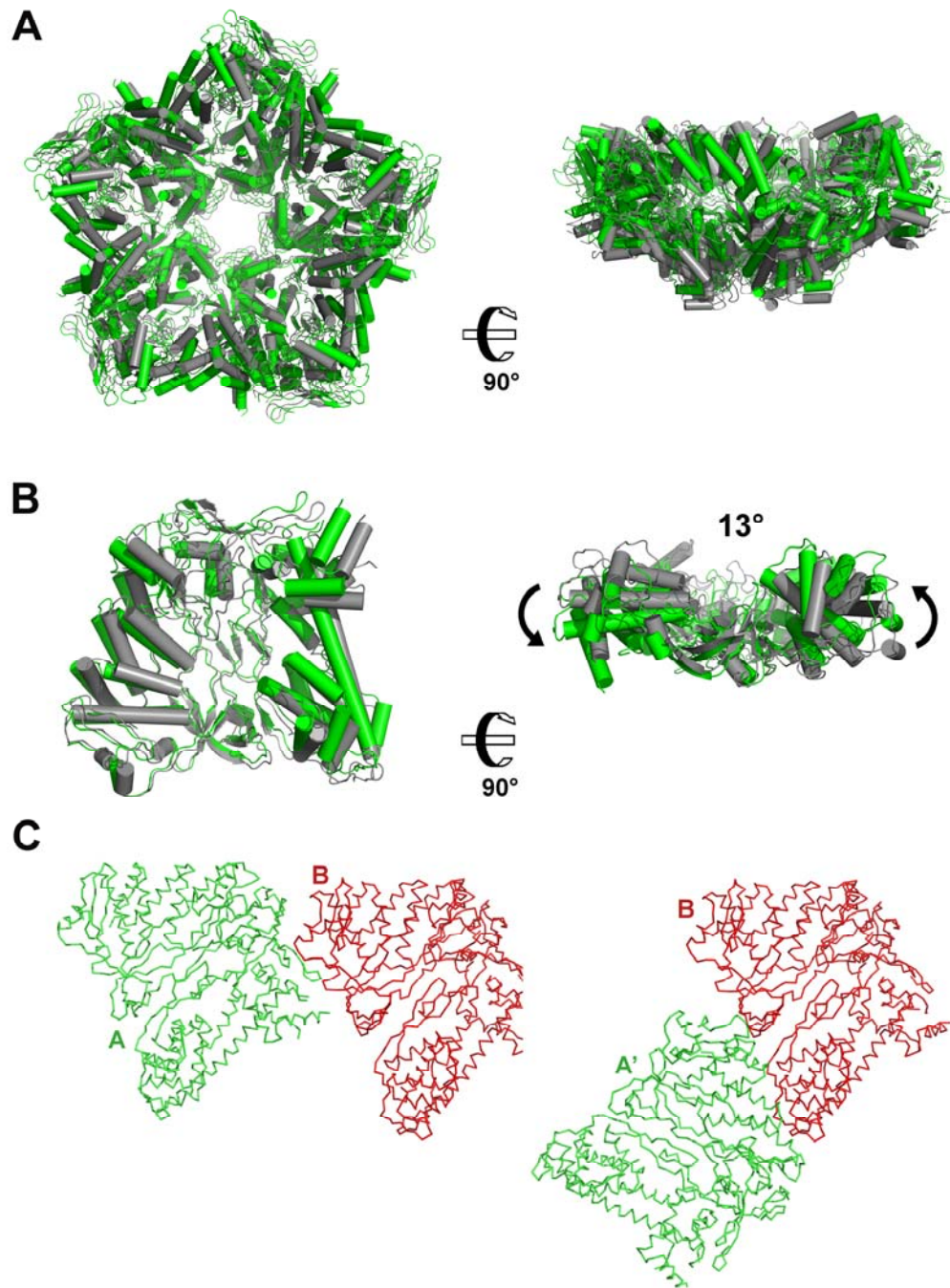
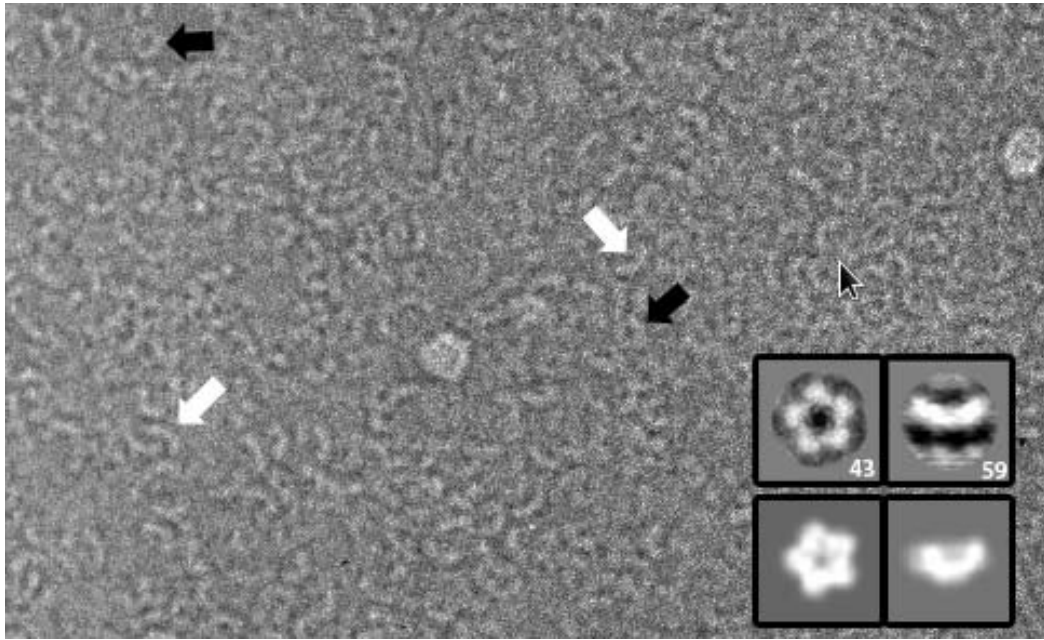


Figure S3



**Figure S4**

## FIGURE LEGENDS

**Figure S1:** Crystal packing the  $\phi 8$  P1 pentamers, related to Figure 1. On the left, ribbon representation of the pentamers in the crystal. The box represents a close-up view of a slice cut through the middle of two pentamers showing. On the right, model showing the arrangement of the lines formed by the pentamers in the crystal.

**Figure S2:** Representative 2fo-fc electron density map of  $\phi 8$  P1 contoured at  $1\sigma$ , related to Figure 1.  $\phi 8$  P1 monomer is drawn as cartoon and as sticks in the close-up view.

**Figure S3:** (A, B) Comparison of the crystal structure pentamer (grey) to the procapsid pentamer (green) as obtained by fitting P1 monomers into the 5-fold axis of the  $\phi 6$  procapsid cryo-EM reconstruction. (A) Superimposition of the pentamers shown from a top view (left) and side view (right). (B) Rotation movement observed at the level of monomers. (C) Interactions between A and B subunits; P1 is drawn in a ribbon representation with A, A' in red and B in green. related to Figure 4.

**Figure S4:** Presence of pentamers in solution shown by negative-stain EM, related to Figure 5. Top and side views of the pentamers in solution are indicated by black and white arrows respectively. Lower right panels: 2D analysis of  $\phi 8$  P1 in solution; top and side views class averages obtained with EMAN (with numbers of particles used) and corresponding X-ray crystal structure projections Fourier-low-pass filtered to 25Å.

To visualise P1 under negative-stain EM, a volume of 2.5  $\mu\text{l}$  of P1 (0.5 mg/ml), was applied to glow-discharged carbon-coated copper grids immediately after gel-filtration. Grids were negatively stained with 0.75% uranyl formate. Images were

taken under low-dose conditions ( $\sim 10 \text{ e}^-/\text{\AA}^2$  per exposure) at a nominal magnification of  $59,000\times$  on a Tecnai F30 microscope. Micrographs were digitized using a SCAI scanner (Z/I Imaging) at a step size of  $7 \mu\text{m}$  and binned by a factor of 4, resulting in a pixel size of  $4.74 \text{ \AA}/\text{pixel}$ . 2000 windowed particles were subjected to 10 cycles of reference-free alignment using EMAN.